Environmental Science & Technology

Article

pubs.acs.org/est

Black Carbon Sources Constrained by Observations in the Russian High Arctic

Olga B. Popovicheva,[†] Nikolaos Evangeliou,[*,‡] Konstantinos Eleftheriadis,[§] Athina C. Kalogridis,[§] Nikolay Sitnikov,[⊥] Sabine Eckhardt,[‡] and Andreas Stohl[‡]

[†]Scobeltsyn Institute of Nuclear Physics, Lomonosov Moscow State University (MSU), 119991 Moscow, Russia

[‡]Department of Atmospheric and Climate Research (ATMOS), NILU - Norwegian Institute for Air Research, 2007 Kjeller, Norway

[§]N.C.S.R. "Demokritos", Institute of Nuclear and Radiological Sciences & Technology, Energy & Safety, 15341 Agia Paraskevi, Attiki Greece

[⊥]Central Aerological Observatory (CAO), 141700 Moscow, Russia

Supporting Information

ABSTRACT: Understanding the role of short-lived climate forcers such as black carbon (BC) at high northern latitudes in climate change is hampered by the scarcity of surface observations in the Russian Arctic. In this study, highly time-resolved Equivalent BC (EBC) measurements during a ship campaign in the White, Barents, and Kara Seas in October 2015 are presented. The measured EBC concentrations are compared with BC concentrations simulated with a Lagrangian particle dispersion model coupled with a recently completed global emission inventory to quantify the origin of the Arctic BC. EBC showed increased values (100−400 ng m^{-3}) in the Kara Strait, Kara Sea, and Kola Peninsula and an extremely high concentration (1000 ng m^{-3}) in the White Sea. Assessment of BC origin throughout the expedition showed that gas-flaring emissions from the Yamal−Khanty-Mansiysk and Nenets−Komi regions contributed the most when the ship was close to the Kara Strait, north of 70° N. Near Arkhangelsk (White Sea), biomass burning in mid-latitudes, surface transportation, and residential and commercial combustion from Central and Eastern Europe were found to be important BC sources. The model reproduced observed EBC concentrations efficiently, building credibility in the emission inventory for BC emissions at high northern latitudes.

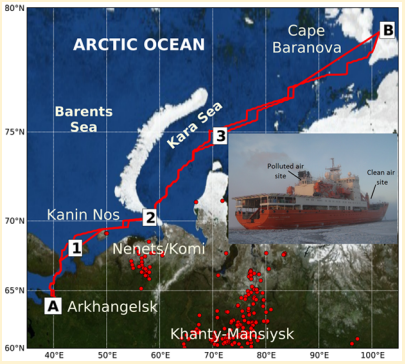

1. INTRODUCTION

Short-lived climate forcers are aerosols and gases that cause radiative forcing[1,2] and have lifetimes of less than a few years.[3,4] Light-absorbing aerosols are of particular interest because they have a warming effect that is strongest over highly reflective surfaces (e.g., clouds, snow, and ice).[5] Furthermore, their deposition on snow and ice decreases surface albedo, which can enhance melting[6,7] and trigger surface warming. Most of the radiation absorption of accumulation-mode aerosol is due to black carbon (BC).[8] BC also influences cloud radiative properties.[9,10] BC originates from incomplete combustion, e.g., of biomass or fossil fuels.[1,11] Freshly emitted BC is hydrophobic but aging in the atmosphere changes its properties to a more-hydrophilic state.[12] It is an important constituent in Arctic Haze, a phenomenon that is primarily the result of long-range pollution transport from sources outside the Arctic.[5,7,13,14] The majority of the Arctic BC originates from anthropogenic sources, especially industrial applications, residential combustion, and diesel transportation activities,[15] while other important sources include fires in boreal forests and agricultural regions especially from spring to fall.[16−18]

Near the surface, about 50% of the BC north of 60° N originates from Russia,[19] where emission inventory data are highly uncertain.[20] Emissions from flaring of gas associated with oil production are prone to particularly high uncertainty because both activity data and emission factors are largely lacking. According to the Global Gas Flaring Reduction Partnership (GGFR) (http://www.worldbank.org/en/programs/gasflaringreduction), nearly 50 billion m^3 of gas are flared in Russia annually. The Russian flaring emissions in the Yamal and Khanty-Mansiysk regions are directly within the major low-altitude pathway of sub-Arctic air masses penetrating into the Arctic,[16] and thus, Stohl et al.[21] estimated that they contribute about 42% of the annual average BC surface concentrations in the Arctic.

However, limited measurements are available that would enable the constraining of this particular source of BC in the Russian Arctic. For instance, in the whole Russian territory north of 50° N, continuous measurements of equivalent BC (EBC) are performed only at Tiksi station (71.36° N; 128.53° E),[22,23] which is far from the major industrial sources in Russia.

Received: November 21, 2016
Revised: February 17, 2017
Accepted: February 24, 2017
Published: February 24, 2017

DOI: 10.1021/acs.est.6b05832
Environ. Sci. Technol. 2017, 51, 3871−3879

Based on isotope measurements, one recent observational study[24] suggests that the contribution of gas flaring emissions to BC at Tiksi is lower than estimated by Stohl et al.[21] However, new bottom-up inventories[25,26] contain gas-flaring emissions that are even higher than those used by Stohl et al.[19] For the clarification of the role of gas-flaring emissions, any EBC measurements from regions closer to the oil production facilities of Russia would be extremely valuable. In these regions, BC has been measured only with low time resolution during a few ship campaigns.[21,27−29] However, to relate such measurements to particular source regions, measurements with high time resolution are necessary. In a comparison with the few available observations, modeled BC concentrations were found to be too low,[21] but a comprehensive analysis was not possible because of the low time resolution of these measurements.

In the present study, we report highly time-resolved EBC concentrations measured during the "Sever-2015" expedition through the White Sea, Barents Sea, and Kara Sea in October 2015. We compare the EBC measurements recorded during the cruise with predicted BC concentrations simulated with a Lagrangian particle dispersion model (LPDM). Furthermore, we investigate and quantify the origin of the BC observed during the cruise using modeling results coupled with the most recent emission inventory for BC. This is done to assess how the oil and gas industrial emissions in high northern latitudes affect Arctic BC.

2. METHODOLOGY

2.1. Expedition and Analysis of Equivalent Black Carbon. The expedition "Sever-2015" was carried out onboard the research vessel "Akademik Treshnikov" of the Russian Arctic and Antarctic Research Institute from October 9 to 25, 2015. The ship is the modern vessel of RMRS (Russian Maritime Register of Shipping, class notation KM Arc7AUT2), and it uses three propulsion WÄRTSILÄ diesel four-stroke engines with 600 rpm. The ship track in the Arctic Ocean and the research vessel are shown in Figure S1, together with the main gas-flaring facilities. The cruise started on October 10 from the port of Arkhangelsk (64.58° N, 40.50° E; point A on the map) and continued through the delta of the Dvina river toward the White Sea and Kanin Nos (point 1 in Figure S 1) in the Barents Sea. Next, it passed the Kara Strait (point 2 in Figure S1) and the Kara Sea until it reached the archipelago Severnaya Zemlya (79.35° N, 101.83° E; point B). After a stay of 2 days near the research station "Ice Base Cape Baranova" on the Bolshevik Island (from October 15 to 17 2015), the ship turned back. A storm forced the ship to moor in the Kara Sea (point 3 in Figure S1) from October 19 to 21 before it could continue its return journey to Arkhangelsk, where it arrived on October 25. Meteorological data (temperature, apparent wind speed, and direction) during the cruise were obtained from the Vaisala maritime observation system MAWS-420. Real wind direction and speed was estimated from the aforementioned data. Surface air temperature, pressure, and wind data are shown in Figure S 2, respectively.

Aerosol EBC concentrations were determined continuously using an aethalometer purposely designed by the Moscow State University (MSU) and Central Aerological Observatory (CAO) for ship campaigns. In this instrument, light attenuation caused by the particles depositing on a quartz fiber filter is measured at three wavelengths (450, 550, and 650 nm). The light-attenuation coefficient of the collected aerosol was calculated with the method of Hansen and Rosen.[30] EBC concentrations were determined continuously by converting the time-resolved light attenuation to the EBC mass corresponding to the same attenuation and characterized by a specific mean mass attenuation coefficient. This calibration parameter was derived during parallel long-term measurements against an AE33 aethalometer (Magee Scientific) that operates at the same three wavelengths (450, 550, and 650 nm).

Attenuation coefficient b_{atn} is defined as

$$b_{atn} = A\ (\mathrm{m}^2)\cdot\delta\mathrm{ATN}/V\ (\mathrm{m}^3) \quad (1)$$

where A is the filter exposed area, V is the volume of air sampled, and δATN is the light attenuation defined as follows:

$$\delta\mathrm{ATN} = \ln(I_o/I) \quad (2)$$

where I_o and I is the light intensity transmitted through unexposed and exposed parts of the filter, respectively. Good linear correlation between the aethalometer's attenuation coefficient b_{atn} and the EBC concentrations calculated with the AE33 aethalometer (at 660 nm) was achieved (R^2 = 0.92; see Figure S3). This allowed the estimation of EBC mass concentrations using the regression slope and intercept between b_{atn} at 650 nm and EBC of the AE33 aethalometer at 660 nm:

$$\mathrm{EBC}\ (\mathrm{ngm}^{-3}) = 3.3\times10^5\cdot A\ (\mathrm{m}^2)\cdot\delta\mathrm{ATN}/V\ (\mathrm{m}^3) \quad (3)$$

where 3.3×10^5 is the correction factor that includes the specific mass absorption coefficient for the MSU aethalometer calibrated against the AE33 aethalometer assuming the mass absorption cross-section (MAC) adopted by AE33 equal to 9.89 $m^2\ g^{-1}$.[31] The uncertainty of EBC measurements from both aethalometers depends on the accuracy of the MAC value used for the conversion of the light-absorption coefficient to mass concentration. The constant MAC value adopted here is an approximation, assuming a uniform state of mixing for BC in atmospheric aerosol. This can be considered a valid assumption in the case of background aerosol measurements performed in this study. Absolute uncertainties of the reported MAC values remain as high as 30−70% due to the lack of appropriate reference methods and calibration materials.[32]

The level of uncertainty (1-σ) of EBC measurements was 30 ng m^{-3} for a 6 min integration time. Aethalometer filters were changed manually at the latest when ATN values approached 70, but at most times, filters were changed at lower values. During rough and wet weather conditions, water droplets or sea spray affected the measurements adding higher noise to the recorded ATN signal. These short data periods were either excluded from the data set or, where possible, treated manually by establishing an adjusted baseline for the reference ATN values.

To identify the cleanest location on the vessel (i.e., the spot least influenced by the ship exhaust), particulate mass (PM) concentration was measured on all decks of the vessel using a TSI DustTrak 8530 monitor. The best site for ambient aerosol monitoring was identified to be at the foredeck, where the aethalometer was placed, while the spot most affected by the exhaust pipe was found at about 10 m on the upper bridge (Figure S 1). A second aethalometer of exactly the same type was therefore installed at this location to record potential impact from ship pollution. EBC concentrations from the two aethalometers were compared and the absence of contamination on the foredeck, where the aethalometer was placed

DOI: 10.1021/acs.est.6b05832
Environ. Sci. Technol. 2017, 51, 3871−3879

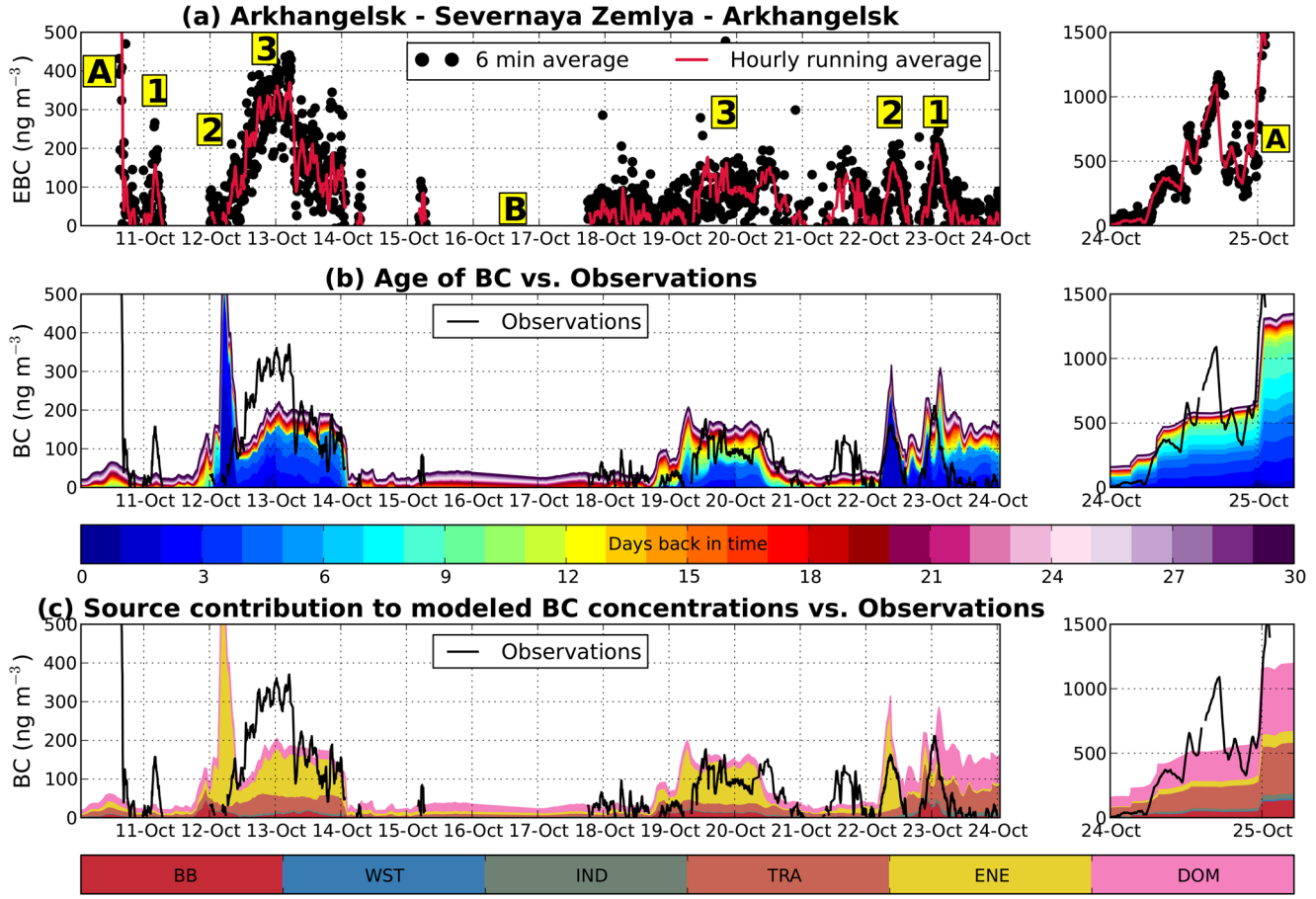

Figure 1. (a) Time series of equivalent black carbon (EBC) mass concentrations during the expedition cruise. Numbers and letters in red brackets show geographical names during the cruise according to Figure S1. (b) Age spectra of modeled BC (colors) from all possible sources showing the contribution of emissions each day back in time to the surface concentration of BC. Hourly means of measured BC concentrations are shown as a black line. (c) Contribution from different emission source types to the BC surface concentrations. The emission sources of biomass burning (BB); waste burning (WST); industrial combustion and processing (IND); surface transportation (TRA); power plants, energy conversion, and extraction (ENE); and residential and commercial (DOM) have been adopted from GFEDv3.1 and ECLIPSE inventories.[36,37] Notice that the different scale used in all three panels from October 24th to the 25th, when measured and modeled concentrations were much higher than for the rest of the cruise. Flaring emissions are included in the energy sector (ENE).

(clean air site), was assured. When the apparent wind was blowing from the back of the vessel toward the clean air site on the foredeck, all aethalometer data were removed from further analysis. For instance, such contamination might have occurred when the ship moored near point 3 (Figure S1) during the storm event, and therefore, these measurements were removed from the data set.

2.2. Emissions and Modeling of Black Carbon. The concentrations of BC were simulated with version 10 of the flexible particle dispersion model (LPDM FLEXPART).[33,34] The model was driven with operational meteorological analyses every 3 h from the European Centre for Medium-Range Weather Forecasts (ECMWF). The ECMWF data had 137 vertical levels and a horizontal resolution of 1° × 1°. Computational particles released from the measurement locations were tracked back in time in FLEXPART's "retroplume" mode.[35] Simulations extended over 30 days back in time, sufficient to include most aerosol emissions arriving at the station, given a typical BC lifetime (~1 week). This enabled the identification of where the measured BC came from and allowed the quantification of BC source contributions. The source contributions can also be displayed as a function of the time elapsed since the emission has occurred (i.e., "age"), which can be shown as "age spectrum" consisting of stacked bars, where a bar's color indicates the contribution of a certain age bin (0−1 days, 1−2 days...29−30 days) (see Figure 1b). FLEXPART simulations were performed every hour during the cruise, with particles released from small boxes covering the latitude and longitude ranges of the ship track during the hour. The FLEXPART retroplumes consist of an emission sensitivity (often also called source-receptor relationship), which yields a simulated concentration in the receptor box when multiplied with gridded emissions from an inventory.

Emission fluxes were taken from the "Evaluating the CLimate and Air Quality ImPacts of ShortlivEd Pollutants" (ECLIPSE) version 5 emission data set,[36] which is available from the Web site of the International Institute for Applied Systems Analysis (IIASA) (http://www.iiasa.ac.at/web/home/research/researchPrograms/air/Global_emissions.html). This inventory is appropriate for use in our study, as it accounts for BC emissions from gas flaring from the main emitting facilities located west of Yamal Peninsula (Komi and Nenets distinct) and in Khanty-Mansiysk (south of Yamal Peninsula).[21] Biomass burning (BB) sources (namely forest, peat, savanna, woodland fires, and deforestation) were adopted from the Global Fire Emissions Database version 3 (GFED v3.1).[37] With regard to

DOI: 10.1021/acs.est.6b05832
Environ. Sci. Technol. 2017, 51, 3871−3879

anthropogenic sources, it includes industrial combustion and processes sector (IND) emissions from combustion happening in industrial boilers as well as emissions from industrial production processes. Residential and commercial sector (DOM) includes emissions from combustion in heating and cooking stoves and boilers in households and public and commercial buildings like malls, hospitals, and schools. The waste treatment and disposal sector (WST) includes emissions from waste incineration and the treatment process. The transport sector (TRA) includes emissions from all land-based transport of goods, animals and persons on road networks as well as off-road activities, e.g., on railroads, agricultural and forest lands, and construction sites. Shipping in in-land waters and domestic aviation are also included in this sector, but international shipping and aviation are treated as separate sectors. Finally, energy production and distribution sector (ENE) includes emissions from combustion processes in power plants and generators and emission related to distribution of energy to consumers, as well as emissions from gas flaring in oil facilities.

For our simulations, we assumed that BC has a density of 2000 kg m^{-3} and follows a logarithmic size distribution with an aerodynamic mean diameter of 0.25 μm and a logarithmic standard deviation of 0.3. Each computational particle released in FLEXPART represents an aerosol population with a log-normal size distribution.[34] This treatment of aerosol size distribution allows the simulation of several different types of particles, each with its own size distribution. Removal processes acting differently for the different particle sizes will then affect specific particle sizes. Assumed aerodynamic mean diameter and logarithmic standard deviation are used by FLEXPART's dry deposition scheme, which is based on the resistance analogy,[38] and they are consistent with those used in other transport models.[18,39] Below-cloud scavenging was determined based on the precipitation rate taken from ECMWF. The in-cloud scavenging was based on cloud liquid water and ice content, precipitation rate, and cloud depth from ECMWF.[40] The FLEXPART user manual (available from http://www.flexpart.eu) provides more information on FLEXPART's removal parametrizations. All FLEXPART results for the cruise can be viewed interactively at http://niflheim.nilu.no/NikolaosPY/RusArctExp_2015.py.

3. RESULTS AND DISCUSSION

3.1. Onboard EBC Measurements. The EBC concentrations measured during the cruise are shown in Figure 1a. At the beginning of the expedition (October 10, 2015) when the ship was in or near the port of Arkhangelsk (White Sea), high values of EBC were measured (hourly values up to 700 ng m^{-3}), probably due to local pollution. Only after the ship passed the industrial area of the Dvina river delta (October 10, 2015 at 20:30), EBC dropped to below 100 ng m^{-3}. In the open White Sea, EBC was 40 ng m^{-3}, on average, but a small peak (~163 ng m^{-3}) was observed near the Kola Peninsula in the morning of October 11 (06:30). In the basin of the Barents Sea absorption was below the detection limit of the aethalometer, and only in the Pechora Sea (West of Kara Strait) on October 12 (06:30) did EBC concentrations rise above the minimum detection levels again, gradually increasing up to 153 ng m^{-3}. In the Kara Strait EBC was strongly enhanced (~220 ng m^{-3}); concentrations kept increasing in the Kara Sea up to a maximum of 360 ng m^{-3} (Figure 1a), in an area north of strong gas-flaring emissions (see Figure 1 in ref 21). Notice that at remote Arctic stations, measured EBC concentrations are much lower, typically only around 10 ng m^{-3} at this time of the year,[41] which can be considered the typical Arctic background.[42] Hence, EBC values observed in the Barents Sea were relatively close to the background concentrations observed in other parts of the Arctic, whereas in the Kara Sea, EBC concentrations were strongly enhanced compared to this level. It is worth to note that the measured EBC concentrations are comparable to those reported by Stohl et al.[21] of about 200−400 ng m^{-3} during a ship cruise in the Kara Sea in September of 2011.

In the morning of October 13 (07:30), when the ship was in the Eastern Kara Sea, EBC dropped to 100 ng m^{-3} and then varied between 50 and 220 ng m^{-3} until midnight of October 14 before decreasing toward minimum detectable limits until archipelago Severnaya Zemlya. On October 15 (02:50), the ship moored in the Shokalsky's passage near station "Ice Base Cape Baranova" on the Bolshevik Island (Figure S 1) until October 18, when the voyage back to Arkhangelsk started.

On the way back to Arkhangelsk, on the morning of October 18, we observed EBC concentrations reaching around 60 ng m^{-3} (Figure 1a). While these concentrations were lower than those observed on the way to the Bolshevik Island, they are still much higher than the Arctic background. From October 19 at 10:00 to October 21 at 22:00, the ship maneuvered in the central part of the Kara Sea searching for mooring stations. At that time BC varied to about 200 ng m^{-3}. However, due to frequent changes of the ship's course, the ship's exhaust might have been transported to the clean air site (see Figure S1) via complicated pathways. Therefore, enhanced EBC measurements during this period were excluded from further analysis. On October 21, when the vessel continued its voyage to Arkhangelsk, relatively high EBC concentrations were measured, while on October 22 at 18:00, no absorption could be measured. On October 23, the ship passed through the Kara Strait recording EBC concentrations of up to 250 ng m^{-3}. Measured EBC concentrations declined substantially in the Barents Sea until the ship reached the Kola Peninsula, where a small peak was recorded on October 24 at around 6:00. Next, EBC rapidly increased along the Dvina River in the White Sea with a maximum of about 1100 ng m^{-3} on October 24 and 25, 2015. When the ship arrived at the port of Arkhangelsk, EBC concentrations of 1500 ng m^{-3} were measured. Although we initially considered these high EBC concentrations close to the port of Arkhangelsk as local pollution, in the next section, we show that this was actually not the case.

3.2. Analysis of BC Sources Observed during the Expedition. Figure 1b shows the modeled concentrations color-coded according to their age since emission in contrast to the measurements, while in Figure 1c, the modeled concentrations are separated according to the different emission categories. It was already mentioned that the ECLIPSE inventory includes anthropogenic and biomass burning emission sources adopted from GFED v3.1.[36,37] Flaring emissions dominate the emissions from the energy (ENE) sector south of the Barents and Kara Seas. Generally, the model captured periods with enhanced concentrations (e.g., in the Kara Sea during both the outward and return trip) and such with very low concentrations (e.g., in the Barents Sea) quite well. One exception is the first few hours of the cruise, when FLEXPART retroplumes showed that clean air masses from the Arctic reached the vessel in the port of Arkhangelsk. It is, however, very likely that the high measured EBC concen-

DOI: 10.1021/acs.est.6b05832
Environ. Sci. Technol. 2017, 51, 3871−3879

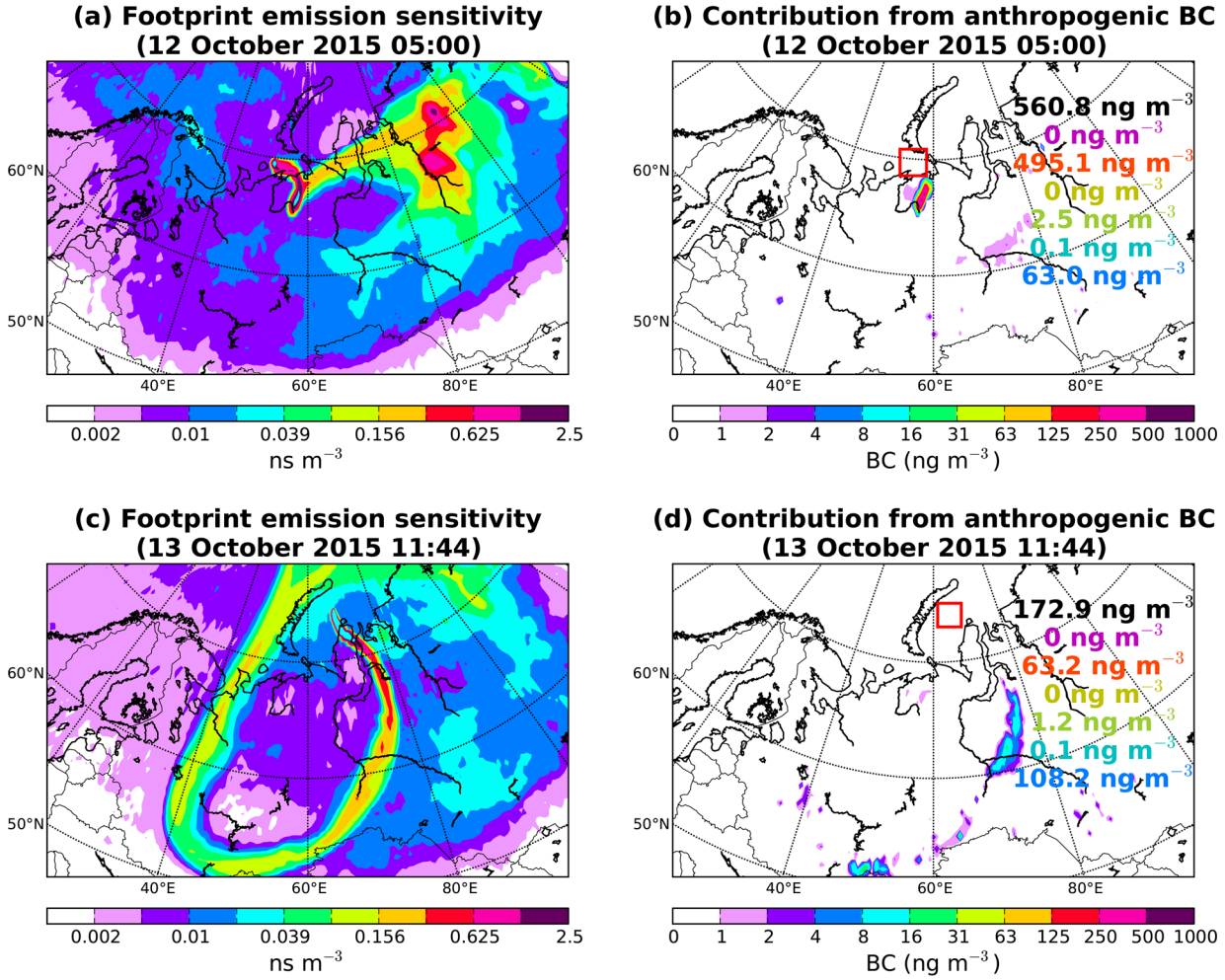

Figure 2. (a) Footprint emission sensitivity and (b) contribution from anthropogenic sources to surface BC concentrations on October 12, 2015 at 05:00. (c) Footprint emission sensitivity and (d) contribution from anthropogenic sources to surface BC concentrations on October 13, 2015 at 11:44. Values written in black report the simulated concentration of BC at the receptor (ship) for the same time period from all anthropogenic sources, while colored ones denote the continental contribution from anthropogenic sources. Magenta areas show contribution from South America, orange from Europe, yellow from Australia, green from North America, cyan from Africa, and blue from Asia.

trations were caused exclusively by local pollution within the port, which cannot be captured by FLEXPART.

In the morning of October 12, FLEXPART strongly overestimated the measured BC concentrations (shortly before the ship passed through the Kara Strait), then underestimated them by about 50% and finally captured them almost exactly in the Kara Sea (October 13). As shown in Figure 1c, the modeled concentrations during this period had a large flaring contribution (ENE in Figure 1c). The measurements during this period thus enable us to constrain the rather uncertain gas-flaring emissions. Before the highest modeled BC peak on October 12, retroplumes arrived straight from the east, with very little influence from the continent. At the time of the model peak, however, the retroplume encountered the northern parts of a strong cyclone centered over the Urals during the previous days. As a consequence, the retroplume turned direction over the Nenets and Komi regions almost exactly where the ECLIPSE inventory places very high gas-flaring emissions, resulting in very high values of the footprint emission sensitivity (Figure 2a) and source contributions (Figure 1c). This complex situation prevailed only for about 3 h. After that, the retroplume circled the whole cyclone and this situation prevailed constantly for more than a day and during the entire passage of the Kara Sea (see Figures 2c and 3d). Based on the above analysis, it is likely that the modeled BC peak on October 12 is a result of the model not capturing the complex meteorological situation accurately enough. Even a small shift in the location of where the retroplume turned (Figure 2a) would have produced much smaller simulated BC concentrations. When the meteorological situation was more stable, the model captured the measured EBC concentrations rather well, especially on October 13, when gas flaring emissions from the Yamal and Khanty-Mansiysk region contributed strongly. This suggests that gas flaring emissions for this region in the ECLIPSE inventory are in the right order of magnitude, perhaps with a slight tendency toward overestimation in the Nenets and Komi regions.

The very small EBC values in the Severnaya Zemlya archipelago were also well captured by FLEXPART (Figure 1b). During this time, the retroplumes showed transport from the Arctic Ocean, with very little influence from land sources. Figure 3a,b depicts FLEXPART daily average emission sensitivities calculated when the vessel arrived to Severnaya Zemlya (October 14, 2015) and when it departed (October 18, 2015). Winds shifted on October 18, with retroplumes arriving again first from southerly directions and thus increasing the

DOI: 10.1021/acs.est.6b05832
Environ. Sci. Technol. 2017, 51, 3871−3879

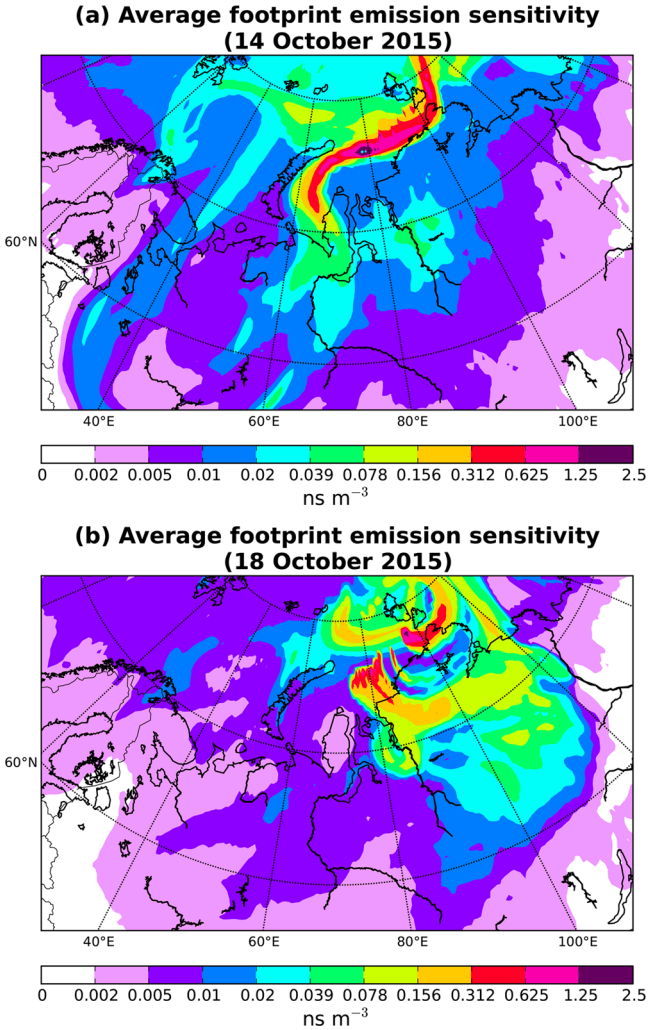

Figure 3. Daily average footprint emission sensitivities when the vessel (a) arrived (October 14, 2015) and (b) departed (October 18, 2015) from the "Ice Base Cape Baranova" station.

potential for BC uptake over the land. Indeed, both measured and modeled BC concentrations increased again on October 18.

On the way back, measured EBC concentrations in the Kara Sea were again captured quite accurately by FLEXPART. On October 19 to 20, BC originated mainly from the Russian gas flaring sites of Yamal and Khanty-Mansiysk, confirming that these emissions appear to be well-captured by the ECLIPSE inventory. From the afternoon on October 20, air arrived straight from the west and was not influenced anymore by sources on the continent. This was also the case on October 21, when air came from the north. Measurements also showed decreasing EBC concentrations from October 20 to 21 (from 135 ng m^{-3} on October 20 at 10:00 to near the detection limit on October 21 at 2:00).

On October 22, as the ship approached the Kara Strait, air arrived from the southwest and gas flaring emissions from the Nenets and Komi regions were sampled again, similar to the results from October 12. This time, the model overestimated the measured EBC concentrations only slightly. Nevertheless, together with the results from the outward journey, this may suggest that flaring emissions in the Nenets and Komi regions are somewhat overestimated in the ECLIPSE inventory.

On October 24 to 25, measured EBC values in the White Sea reached more than 1000 ng m^{-3} and FLEXPART simulated similarly high BC values. The retroplumes at this time arrived from the southwest and brought polluted air masses mainly from Eastern Europe (Figure 4a). An example of the source contributions for October 25 at 00:00 is shown in Figures 4b and 5c. At that time, the modeled concentration of BC was 1310.5 ng m^{-3}, which is close to the observed values in the range from 696 to 1501 ng m^{-3}. About 10% (130.8 ng m^{-3}) originated from fires over Ukraine (Figure 4c), whereas about 90% originated from anthropogenic sources mainly in Central and Eastern Europe (Figure 4b). Excluding biomass burning, surface transportation contributed about 38%, residential and commercial combustion sources up to 41%, gas flaring contributed about 8%, and emissions from industrial combustion and processing contributed between 1−2%.

Figure 5 depicts calculated normalized bias for the daily average measured EBC and modeled BC concentrations along the ship track in the White, Barents, and Kara Seas. This statistic expresses the difference (model-observed) over the observed values. It is a useful indicator for assessing the models' performance because it avoids overinflating the observed range of values, especially at low concentrations, and it is used here to show the locations where modeled concentrations over- or underestimated the observations. The model is least biased when the gas-flaring sources contribute the most to surface concentrations of BC, namely in the Pechora Sea (west of Kara Sea), in the Kara Strait, and in the Kara Sea on the way to the Bolshevik Island, as well as in the middle of the Kara Sea (point 3 in Figure S1), and close to the port of Arkhangelsk on the way back to Arkhangelsk. The extremely low concentrations calculated by the model in the beginning of the cruise in contrast to the high EBC concentrations (≈700 ng m^{-3}) led to negative biases near the port of Arkhangelsk and in the industrial area of Dvina river delta. On the contrary, the lack of absorption in the aethalometer near the Bolshevik Island from October 15 to 17 resulted in significant overestimated BC concentrations predicted by the model and high positive biases (Figure 5).

The very good agreement (R^2 = 0.76) between modeled and measured concentrations was confirmed by the root-mean-square error (RMSE). Whereas R^2 is a relative measure of fit, RMSE is an absolute measure of fit. It can be interpreted as the standard deviation of the unexplained variance; hence it is in the same units as the response variable. Lower values of RMSE indicate better fit. RMSE is a good measure of how accurately the model predicts the response, and is the most important criterion for fit if the main purpose of the model is prediction. The RMSE, when all data were included, was estimated to be 230 ng m^{-3}. This high value is more or less expected here considering that the RMSE calculates the square error, hence it is very sensitive to larger errors. In the present case, if the points from the initial period of the cruise (Arkhangelsk and Dvina river industrial area) that were subject to local pollution are excluded, the RMSE falls to 85 ng m^{-3}, which is very low compared to the range of values observed during the cruise (0−1500 ng m^{-3}).

Overall, we found that the model had no systematic bias compared to the observations, which supports the validity of the ECLIPSE emission inventory for northern Russia. The good agreement, especially in the region where flaring emissions are important, suggests that flaring emissions are also captured quite well in this inventory. This is particularly

DOI: 10.1021/acs.est.6b05832
Environ. Sci. Technol. 2017, 51, 3871−3879

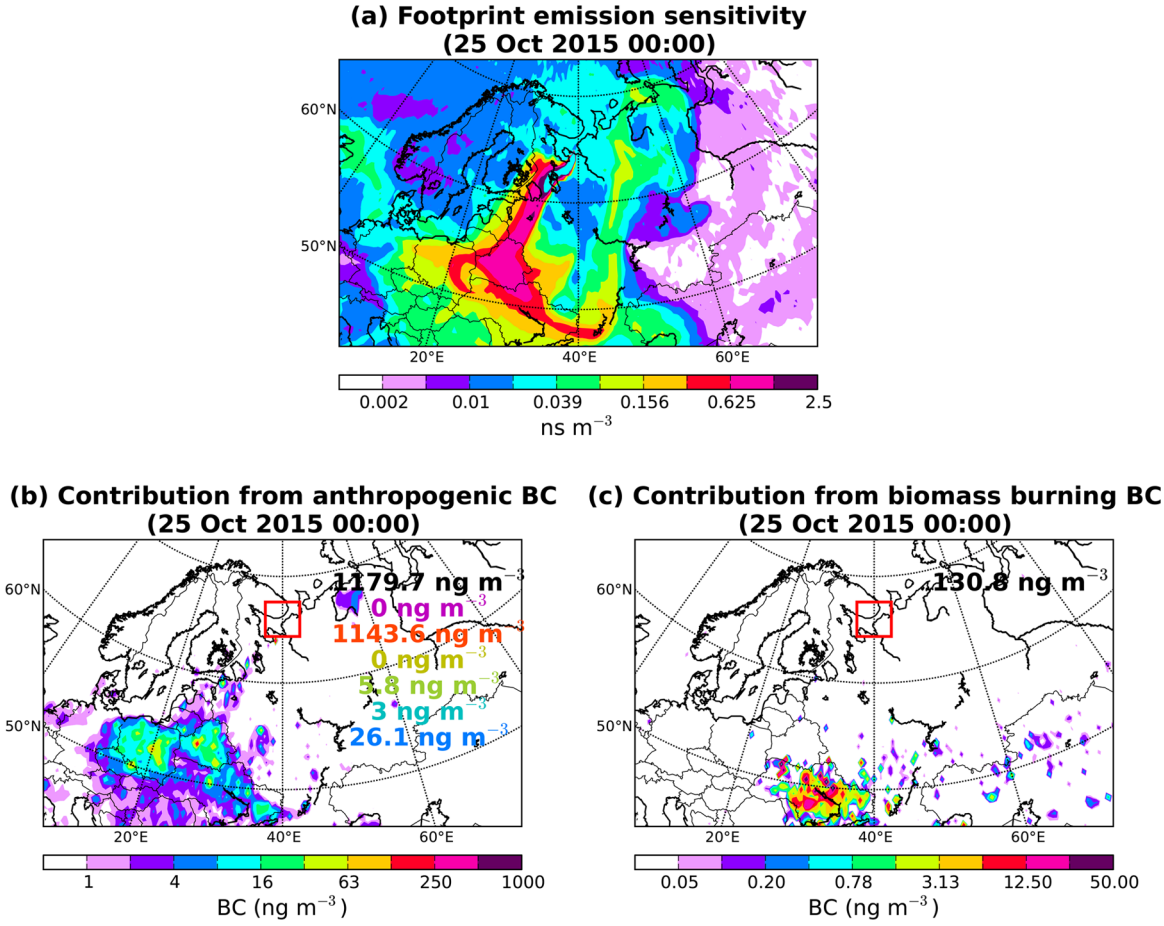

Figure 4. (a) Footprint emission sensitivity when the ship had passed the Dvina River and before arrival to the port of Arkhangelsk (October 25, 2015 at 00:00). (b) Contribution from anthropogenic sources and (c) biomass burning to the simulated surface concentration of BC at the same date and time. Black values show the concentration of BC at the receptor (ship) for the time period from all anthropogenic- and biomass-burning sources. Colored values denote continental contribution from anthropogenic sources; magenta areas show contribution from South America, orange from Europe, yellow from Australia, green from North America, cyan from Africa, and blue from Asia.

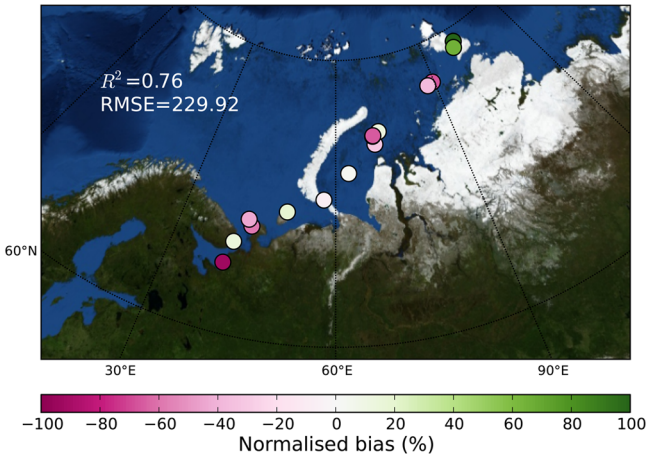

Figure 5. Distribution of normalized bias, i.e., modeled-observed over observed, for the measured EBC and the BC concentrations predicted by FLEXPART. The biases were calculated for the daily average concentrations and for the ship location at midnight of each day (00:00).

true for the Yamal and Khanty-Mansiysk regions, whereas there may be some overestimation of flaring emissions in the Nenets and Komi regions. Local pollution cannot be captured by our model due to poor temporal and spatial resolution of the available operational wind fields or by the emission inventory used (available in 0.5° resolution). When local pollution was insignificant (e.g., in regions far from urban and industrial areas), emissions from residential and commercial combustion, as well as surface transportation, were also captured well.

■ ASSOCIATED CONTENT

Supporting Information

The Supporting Information is available free of charge on the ACS Publications website at DOI: 10.1021/acs.est.6b05832.

Figures show the ship track of the research vessel "Akademik Treshnikov" in the Arctic Ocean and the main flaring facilities located in high latitudes, the measured meteorological conditions during cruise (namely, surface air temperature and pressure and wind velocity and direction), and the quality of the EBC measurements (QA/QC) in terms of comparison of attenuation coefficients of the aethalometers used onboard (MSU) against EBC concentrations obtained with the AE33 aethalometer. (PDF)

DOI: 10.1021/acs.est.6b05832
Environ. Sci. Technol. 2017, 51, 3871−3879

AUTHOR INFORMATION

Corresponding Author

*Phone: +47 63 89 81 89; fax: +47 63 89 80 50; e-mail: Nikolaos.Evangeliou@nilu.no.

ORCID

Nikolaos Evangeliou: 0000-0001-7196-1018

Notes

The authors declare no competing financial interest.

ACKNOWLEDGMENTS

The authors thank the expedition leader V.T. Sokolov for his support. Financial support from RFBR-VAST 15-5554020 is kindly appreciated. We also acknowledge the project entitled "Emissions of Short-Lived Climate Forcers near and in the Arctic (SLICFONIA)", which is funded by the NORRUSS research program of the Research Council of Norway (Project ID: 233642). Finally, we thank IIASA (especially Chris Heyes and Zig Klimont) for providing the BC emission dataset. The data used can be accessed upon request to the corresponding author of this manuscript.

REFERENCES

(1) Bond, T. C.; Doherty, S. J.; Fahey, D. W.; Forster, P. M.; Berntsen, T.; Deangelo, B. J.; Flanner, M. G.; Ghan, S.; Kärcher, B.; Koch, D.; et al. Bounding the role of black carbon in the climate system: A scientific assessment. *J. Geophys. Res. Atmos.* **2013**, *118* (11), 5380−5552.

(2) IPCC. *Climate Change 2013: The Physical Science Basis. Contribution to the Fifth Assessment Report of the Intergovernmental Panel on Climate Change.*; Stocker, T. F., Qin, D., Plattner, G.-K., Tignor, M. M. B., Allen, S. K., Boschung, J., Nauels, A., Xia, Y., Bex, V., Midgley, P. M., Eds.; Cambridge University Press: Cambridge, U.K., 2013.

(3) Shindell, D. T.; Chin, M.; Dentener, F.; Doherty, R. M.; Faluvegi, G.; Fiore, A. M.; Hess, P.; Koch, D. M.; MacKenzie, I. A.; Sanderson, M. G.; et al. A multi-model assessment of pollution transport to the Arctic. *Atmos. Chem. Phys.* **2008**, *8*, 5353−5372.

(4) Bowerman, N. H. A.; Frame, D. J.; Huntingford, C.; Lowe, J. A.; Smith, S. M.; Allen, M. R. The role of short-lived climate pollutants in meeting temperature goals. *Nat. Clim. Change* **2013**, *3* (12), 1021−1024.

(5) Quinn, P. K.; Bates, T. S.; Baum, E.; Doubleday, N.; Fiore, A. M.; Flanner, M.; Fridlind, A.; Garrett, T. J.; Koch, D.; Menon, S.; et al. Short-lived pollutants in the Arctic: their climate impact and possible mitigation strategies. *Atmos. Chem. Phys.* **2008**, *8*, 1723−1735.

(6) Warren, S. G.; Wiscombe, W. J. A Model for the Spectral Albedo of Snow. II: Snow Containing Atmospheric Aerosols. *J. Atmos. Sci.* **1980**, *37*, 2734−2745.

(7) Flanner, M. G.; Zender, C. S.; Randerson, J. T.; Rasch, P. J. Present-day climate forcing and response from black carbon in snow. *J. Geophys. Res.* **2007**, *112* (11), 1−17.

(8) Petzold, A.; Ogren, J. A.; Fiebig, M.; Laj, P.; Li, S. M.; Baltensperger, U.; Holzer-Popp, T.; Kinne, S.; Pappalardo, G.; Sugimoto, N.; et al. Recommendations for reporting black carbon measurements. *Atmos. Chem. Phys.* **2013**, *13* (16), 8365−8379.

(9) Popovicheva, O. B. Combustion-derived carbonaceous aerosols (soot) in the atmosphere: Water interaction and climate effects. In *Aerosol Sci. Technol.*; Agranovski, I., Ed.; Wiley - VCH Verlag GmbH & Co. KGaA: Weinheim, Germany, 2010; pp 127−157.

(10) Yun, Y.; Penner, J. E.; Popovicheva, O. The effects of hygroscopicity on ice nucleation of fossil fuel combustion aerosols in mixed-phase clouds. *Atmos. Chem. Phys.* **2013**, *13* (8), 4339−4348.

(11) Popovicheva, O.; Kistler, M.; Kireeva, E.; Persiantseva, N.; Timofeev, M.; Kopeikin, V.; Kasper-Giebl, A. Physicochemical characterization of smoke aerosol during large-scale wildfires: Extreme event of August 2010 in Moscow. *Atmos. Environ.* **2014**, *96* (2014), 405−414.

(12) Diapouli, E.; Popovicheva, O.; Kistler, M.; Vratolis, S.; Persiantseva, N.; Timofeev, M.; Kasper-Giebl, A.; Eleftheriadis, K. Physicochemical characterization of aged biomass burning aerosol after long-range transport to Greece from large scale wildfires in Russia and surrounding regions, Summer 2010. *Atmos. Environ.* **2014**, *96*, 393−404.

(13) Eleftheriadis, K.; Vratolis, S.; Nyeki, S. Aerosol black carbon in the European Arctic: Measurements at Zeppelin station, Ny-Ålesund, Svalbard from 1998−2007. *Geophys. Res. Lett.* **2009**, *36* (2), 1−5.

(14) AMAP. *AMAP assessment 2015: Black carbon and ozone as Arctic climate forcers*; Arctic Monitoring and Assessment Programme (AMAP), Oslo, Norway, 2015.

(15) Wang, Q.; Chen, X. Nuclear accident like Fukushima unlikely in the rest of the world? *Environ. Sci. Technol.* **2011**, *45* (23), 9831−9832.

(16) Stohl, A.; Berg, T.; Burkhart, J. F.; Fjæraa, A. M.; Forster, C.; Herber, A.; Hov, Ø.; Lunder, C.; McMillan, W. W.; Oltmans, S.; et al. Arctic smoke & record high air pollution levels in the European Arctic due to agricultural fires in Eastern Europe in spring 2006. *Atmos. Chem. Phys.* **2007**, *7* (2), 511−534.

(17) Stock, M.; Ritter, C.; Herber, A.; von Hoyningen-Huene, W.; Baibakov, K.; Gräser, J.; Orgis, T.; Treffeisen, R.; Zinoviev, N.; Makshtas, A.; et al. Springtime Arctic aerosol: Smoke versus haze, a case study for March 2008. *Atmos. Environ.* **2012**, *52* (2012), 48−55.

(18) Evangeliou, N.; Balkanski, Y.; Hao, W. M.; Petkov, A.; Silverstein, R. P.; Corley, R.; Nordgren, B. L.; Urbanski, S. P.; Eckhardt, S.; Stohl, A.; et al. Wildfires in northern Eurasia affect the budget of black carbon in the Arctic-a 12-year retrospective synopsis (2002−2013). *Atmos. Chem. Phys.* **2016**, *16* (12), 7587−7604.

(19) AMAP. *The Impact of Black Carbon on Arctic Climate*; Berntsen, T., Burkhart, J. F., Christensen, J., Flanner, M., Kupiainen, K., Lihavainen, H., Shepherd, M., Shevchenko, V., Skov, H., Vestreng, V., Eds.; Arctic Monitoring and Assessment Programme (AMAP), Oslo, Norway, 2011; Vol. 4.

(20) Cofala, J.; Amann, M.; Klimont, Z.; Kupiainen, K.; Höglund-Isaksson, L. Scenarios of global anthropogenic emissions of air pollutants and methane until 2030. *Atmos. Environ.* **2007**, *41* (38), 8486−8499.

(21) Stohl, A.; Klimont, Z.; Eckhardt, S.; Kupiainen, K.; Shevchenko, V. P.; Kopeikin, V. M.; Novigatsky, A. N. Black carbon in the Arctic: The underestimated role of gas flaring and residential combustion emissions. *Atmos. Chem. Phys.* **2013**, *13* (17), 8833−8855.

(22) Cheng, M. D. Geolocating Russian sources for Arctic black carbon. *Atmos. Environ.* **2014**, *92*, 398−410.

(23) Uttal, T.; Makshtas, A.; Laurila, T. The Tiksi International Hydrometeorological Observatory - An Arctic Members Partnership. *Bull. World Meteorol. Organ.* **2013**, *62* (1), 22−26.

(24) Winiger, P.; Andersson, A.; Eckhardt, S.; Stohl, A.; Semiletov, I. P.; Dudarev, O. V.; Charkin, A.; Shakhova, N.; Klimont, Z.; Heyes, C.; et al. Siberian Arctic black carbon sources constrained by model and observation. *Proc. Natl. Acad. Sci. U. S. A.* **2017**, *114*, 1054−1061.

(25) Huang, K.; Fu, J. S.; Prikhodko, V. Y.; Storey, J. M.; Romanov, A.; Hodson, E. L.; Cresko, J.; Morozova, I.; Ignatieva, Y.; Cabaniss, J. Russian anthropogenic black carbon: Emission reconstruction and Arctic black carbon simulation. *J. Geophys. Res. Atmos.* **2015**, *120* (21), 11306−11333.

(26) Huang, K.; Fu, J. S. A global gas fl aring black carbon emission rate dataset from 1994 to 2012. *Nature* **2016**, 1−11.

(27) Panchenko, M. V.; Kozlov, V. S.; Pol'kin, V. V.; Golobokova, L. P.; Pogodaeva, T. V.; Khodzher, T. V.; Lisitzin, A. P.; Shevchenko, V. P. Investigations of microphysical and chemical composition of aerosol in near-water layer of the atmosphere over the White Sea. *Proc. SPIE* **2012**, *66221A*.65221A10.1117/12.723164

(28) Kopeikin, V. M.; Repina, I. A.; Grechko, E. I.; Ogorodnikov, B. I. Measurements of soot aerosol content in the near-water atmospheric layer in the southern and northern hemispheres. *Atmos. Oceanic Opt.* **2010**, *23* (6), 500−507.

DOI: 10.1021/acs.est.6b05832
Environ. Sci. Technol. 2017, 51, 3871−3879

(29) Sakerin, S. M.; Bobrikov, A. A.; Bukin, O. A.; Golobokova, L. P.; Pol'Kin, V. V.; Pol'Kin, V. V.; Shmirko, K. A.; Kabanov, D. M.; Khodzher, T. V.; Onischuk, N. A.; et al. On measurements of aerosol-gas composition of the atmosphere during two expeditions in 2013 along the Northern Sea Route. *Atmos. Chem. Phys.* **2015**, *15* (21), 12413−12443.
(30) Hansen, A. D. A.; Rosen, H. Horizontal inhomogeneities in the particulate carbon component of the Arctic haze. *Atmos. Environ.* **1985**, *19* (12), 2175−2180.
(31) Drinovec, L.; Močnik, G.; Zotter, P.; Prévôt, A. S. H.; Ruckstuhl, C.; Coz, E.; Rupakheti, M.; Sciare, J.; Müller, T.; Wiedensohler, A.; et al. The "dual-spot" Aethalometer: An improved measurement of aerosol black carbon with real-time loading compensation. *Atmos. Meas. Tech.* **2015**, *8* (5), 1965−1979.
(32) Zanatta, M.; Gysel, M.; Bukowiecki, N.; Muller, T.; Weingartner, E.; Areskoug, H.; Fiebig, M.; Yttri, K. E.; Mihalopoulos, N.; Kouvarakis, G.; et al. A European aerosol phenomenology-5: Climatology of black carbon optical properties at 9 regional background sites across Europe. *Atmos. Environ.* **2016**, *145*, 346−364.
(33) Stohl, A.; Hittenberger, M.; Wotawa, G. Validation of the lagrangian particle dispersion model FLEXPART against large-scale tracer experiment data. *Atmos. Environ.* **1998**, *32* (24), 4245−4264.
(34) Stohl, A.; Forster, C.; Frank, A.; Seibert, P.; Wotawa, G. Technical note: The Lagrangian particle dispersion model FLEXPART version 6.2. *Atmos. Chem. Phys.* **2005**, *5* (9), 2461−2474.
(35) Stohl, A.; Forster, C.; Eckhardt, S.; Spichtinger, N.; Huntrieser, H.; Heland, J.; Schlager, H.; Wilhelm, S.; Arnold, F.; Cooper, O. A backward modeling study of intercontinental pollution transport using aircraft measurements. *J. Geophys. Res.* **2003**, *108* (D12), 4370.
(36) Stohl, A.; Aamaas, B.; Amann, M.; Baker, L. H.; Bellouin, N.; Berntsen, T. K.; Boucher, O.; Cherian, R.; Collins, W.; Daskalakis, N.; et al. Evaluating the climate and air quality impacts of short-lived pollutants. *Atmos. Chem. Phys.* **2015**, *15* (18), 10529−10566.
(37) van der Werf, G. R.; Randerson, J. T.; Giglio, L.; Collatz, G. J.; Kasibhatla, P. S.; Arellano, A. F. J. Interannual variability in global biomass burning emissions from 1997 to 2004. *Atmos. Chem. Phys.* **2006**, *6* (11), 3423−3441.
(38) Slinn, W. G. N. Predictions for particle deposition to vegetative canopies. *Atmos. Environ.* **1982**, *16*, 1785−1794.
(39) Shiraiwa, M.; Kondo, Y.; Moteki, N.; Takegawa, N.; Sahu, L. K.; Takami, A.; Hatakeyama, S.; Yonemura, S.; Blake, D. R. Radiative impact of mixing state of black carbon aerosol in Asian outflow. *J. Geophys. Res.* **2008**, *113* (24), 1−13.
(40) Grythe, H.; Kristiansen, N. I.; Groot Zwaaftink, C. D.; Eckhardt, S.; Ström, J.; Tunved, P.; Krejci, R.; Stohl, A. A new aerosol wet removal scheme for the Lagrangian particle model FLEXPART. *Geosci. Model Dev. Discuss.* **2016**, 1−34.
(41) Eckhardt, S.; Quennehen, B.; Olivié, D. J. L.; Berntsen, T. K.; Cherian, R.; Christensen, J. H.; Collins, W.; Crepinsek, S.; Daskalakis, N.; Flanner, M.; et al. Current model capabilities for simulating black carbon and sulfate concentrations in the Arctic atmosphere: A multi-model evaluation using a comprehensive measurement data set. *Atmos. Chem. Phys.* **2015**, *15* (16), 9413−9433.
(42) Stone, R. S.; Sharma, S.; Herber, A.; Eleftheriadis, K.; Nelson, D. W. A characterization of Arctic aerosols on the basis of aerosol optical depth and black carbon measurements. *Elem. Sci. Anthr.* **2014**, *2*, 1−22.

DOI: 10.1021/acs.est.6b05832
Environ. Sci. Technol. 2017, 51, 3871−3879